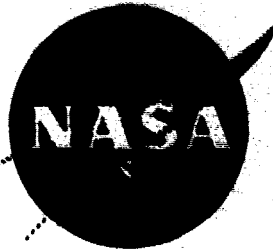


## **General Disclaimer**

### **One or more of the Following Statements may affect this Document**

- This document has been reproduced from the best copy furnished by the organizational source. It is being released in the interest of making available as much information as possible.
- This document may contain data, which exceeds the sheet parameters. It was furnished in this condition by the organizational source and is the best copy available.
- This document may contain tone-on-tone or color graphs, charts and/or pictures, which have been reproduced in black and white.
- This document is paginated as submitted by the original source.
- Portions of this document are not fully legible due to the historical nature of some of the material. However, it is the best reproduction available from the original submission.

NASA CR-134921  
SRD-75-123



# **IMPROVED TOUGHNESS OF SILICON CARBIDE**

(NASA-CR-134921) IMPROVED TOUGHNESS OF  
SILICON CARBIDE Final Report (General  
Electric Co.) 36 p HC \$4.00 CSC

**E76-14270**

by John A. Palm

**GENERAL ELECTRIC COMPANY**  
**CORPORATE RESEARCH AND DEVELOPMENT**

**prepared for**

# NATIONAL AERONAUTICS AND SPACE ADMINISTRATION

**NASA Lewis Research Center  
Contract NAS3-177-7**



## **FINAL REPORT**

November 1975

1. Report No. NASA CR-134921	2. Government Accession No.	3. Recipient's Catalog No.	
4. Title and Subtitle  <b>IMPROVED TOUGHNESS OF SILICON CARBIDE</b>		5. Report Date November 1975	
6. Performing Organization Code			
7. Author(s)  John A. Palm	8. Performing Organization Report No.  SRD-75-123	10. Work Unit No.  YOG 5724	
9. Performing Organization Name and Address  General Electric Company Corporate Research and Development P.O. Box 8 Schenectady, New York 12301	11. Contract or Grant No.  NAS3-17767	13. Type of Report and Period Covered  Final Report	
12. Sponsoring Agency Name and Address  National Aeronautics and Space Administration Washington, D.C. 20546	14. Sponsoring Agency Code		
15. Supplementary Notes  Project Manager, James R. Johnston Materials and Structures Division NASA Lewis Research Center, Cleveland, Ohio			
16. Abstract  Several techniques were employed to apply or otherwise form porous layers of various materials on the surface of hot-pressed silicon carbide ceramic.  From mechanical properties measurements and studies, it was generally concluded that although porous layers could be applied to the silicon carbide ceramic sufficient damage was done to the silicon carbide surface by the processing required so as to drastically reduce its mechanical strength. It was further concluded that there was little, if any, promise of success in forming an effective energy absorbing layer on the surface of already densified silicon carbide ceramic that would, at the same time have the mechanical strength of the untreated or unsurfaced material.  Using the General Electric process for the pressureless sintering of silicon carbide powders, it was discovered that porous layers of silicon carbide could be formed on a dense, strong silicon carbide substrate in a single consolidation process.			
17. Key Words (Suggested by Author(s))  Silicon Carbide Energy Absorbing Surfaces Impact Resistance Pressureless Sintering		18. Distribution Statement  Unclassified - unlimited	
19. Security Classif. (of this report)  Unclassified	20. Security Classif. (of this page)  Unclassified	21. No. of Pages 36	22. Price* \$4.25

\* For sale by the National Technical Information Service, Springfield, Virginia 22151

## **FOREWORD**

The research and development work described in this report was carried out within the Ceramics Branch of the Physical Chemistry Laboratory, at the General Electric Corporate Research and Development Center. It was conducted under National Aeronautics and Space Administration Contract No. NAS3-17767. Mr. James R. Johnston of the National Aeronautics and Space Administration Lewis Research Center was the Contract Manager. Mr. John A. Palm was the principal investigator and Dr. R. J. Charles, Manager of the Ceramics Branch, was Program Manager and Technical Director.

The author acknowledges with thanks the technical assistance provided by W. J. Dondalski, M. J. Curran, J. W. Szymaszek, and the testing and determination of mechanical properties by R. F. Berning and associates. Discussions with Dr. R. J. Charles, Dr. S. Prochazka, Dr. R. Giddings, and Dr. R. Arendt were helpful and appreciated.

## TABLE OF CONTENTS

<u>Section</u>		<u>Page</u>
I	SUMMARY .....	1
II	INTRODUCTION .....	2
III	MATERIALS, PROCEDURES, AND RESULTS.....	4
	A. Base Materials.....	4
	1. Ceralloy 146A.....	4
	2. Hot-pressed Powders GE-IHP Series and PPG (JP #49).....	8
	B. Energy Absorbing Layers (EAL's).....	18
	1. Molten Salt Etch.....	18
	2. Porous Si <sub>3</sub> N <sub>4</sub> on SiC .....	21
	3. Porous Alumina on SiC .....	22
	C. New Approach.....	25
IV	SUMMARY OF RESULTS .....	30
	Appendix A -- HIGH TEMPERATURE CHARPY IMPACT TEST EQUIPMENT	
	Appendix B -- PROJECTILE IMPACT TEST EQUIPMENT	

**PRECEDING PAGE BLANK NOT FILMED**

## LIST OF ILLUSTRATIONS

<u>Figure</u>		<u>Page</u>
1	Ceralloy 146A SiC - polished .....	5
2	SEM Photomicrograph of Ceralloy 146A SiC. Polished and thermal-etched at 1550°C for 20 minutes in Argon. . . . .	5
3	SEM Photomicrograph of Ceralloy 146A SiC. Polished and thermal-etched at 1550°C for 20 minutes in Argon....	6
4	Specimen No. IHPIA Thermal-etched at 1500°C.....	9
5	Specimen No. IHP2. Thermal-etched at 1500°C.....	10
6	Specimen No. IHP 1A-2. Thermal-etched at 1500°C.....	10
7	Specimen No. JP #49. Thermal-etched at 1500°C .....	11
8	Specimen No. IHP3. Thermal-etched at 1500°C .....	11
9	Specimen No. IHP3-A. Thermal-etched at 1500°C.....	12
10	Specimen No. IHP3-B. Thermal-etched at 1500°C.....	12
11	Fracture Surface, Test Specimen No. D (Hot-press JP #49). Charpy Impact Test at 1325°C .....	16
12	Fracture Surface, Test Specimen No. 4/D (Hot-press IHP3). Charpy Impact Test at 1325°C .....	17
13	SEM Photomicrograph of Ceralloy 146A SiC. Treated in a CaCl <sub>2</sub> - CaF <sub>2</sub> - CaSO <sub>4</sub> molten salt bath at 830°C for 30 minutes .....	19
14	SEM Photomicrograph of Ceralloy 146A SiC. Treated in a CaCl <sub>2</sub> - CaF <sub>2</sub> - CaSO <sub>4</sub> molten salt bath at 830°C for 30 minutes .....	20
15	Elemental Si Fusion-bonded to SiC Substrate .....	22
16	Plasma-sprayed Al <sub>2</sub> O <sub>3</sub> Directly Applied Onto SiC Ceramic.....	22
17	Transition Zone Between Dense and Porous SiC by Sintering Two Die-pressed Powders.....	28
18	Transition Zone Between Dense and Porous SiC by Sintering Dipped Layer on Green Compact.....	28
19	Charpy Impact Tester Assembled for Impact Determinations at 1325°C .....	33
20	Base and Portion of Impact Device for Producing Hertzian-type Impact Damage in SiC Surface .....	34

**LIST OF ILLUSTRATIONS (Cont'd)**

<u>Figure</u>		<u>Page</u>
21	Falling Body Projectile Used to Produce Hertzian-type Impact Damage in Silicon Carbide Surface.....	35
22	Strength vs Projectile Impact Loading, Hot-Pressed SiC.....	35

## LIST OF TABLES

<u>Table</u>		<u>Page</u>
I	Three-point Bend Test Fracture Strengths of Ceralloy 146A .....	6
II	Impact Strength of Ceralloy 146A .....	7
III	Surface Profile and Grain Size Measurements of Ceralloy 146A .....	8
IV	Hot-pressed SiC Runs .....	9
V	Charpy Impact Tests on IHPIA and IHP2 Hot-pressed SiC..	13
VI	Three-point Bend Tests on Hot-pressed SiC.....	14
VII	Charpy Impact Tests on Hot-pressed SiC Specimens JP #49 and IHP3 .....	15
VIII	Summary of Average Values of Bend and Charpy Impact Strengths of Hot-pressed SiC Specimens JP #49 and IHP3..	16
IX	Charpy Impact Tests on Hot-pressed SiC Specimens IHP3A and IHP3B .....	17
X	Three-point Bend Test Fracture Strength of Ceralloy 146A after Treatment in CaCl <sub>2</sub> - CaF <sub>2</sub> - CaSO <sub>4</sub> Molten Salt Bath.....	20
XI	Summary of Fracture Strength and Impact Strength of Plasma-Spray-Coated SiC Specimens.....	23
XII	Three-point Bend Tests on Sintered SiC .....	29
XIII	Three-point Bend Strength on Projectile Damaged Specimens.....	36

## ABSTRACT

Several techniques were employed to apply or otherwise form porous layers of various materials on the surface of hot-pressed silicon carbide ceramic.

From mechanical properties measurements and studies, it was generally concluded that although porous layers could be applied to the silicon carbide ceramic sufficient damage was done to the silicon carbide surface by the processing required so as to drastically reduce its mechanical strength. It was further concluded that there was little, if any, promise of success in forming an effective energy absorbing layer on the surface of already densified silicon carbide ceramic that would, at the same time, have the mechanical strength of the untreated or unsurfaced material.

Using the General Electric process for the pressureless sintering of silicon carbide powders, it was discovered that porous layers of silicon carbide could be formed on a dense, strong silicon carbide substrate in a single consolidation process.

**PRECEDING PAGE BLANK NOT FILMED**

## I. SUMMARY

The objective of this program was to develop material systems and the processing procedures which would significantly improve the toughness of silicon carbide refractory compounds. The approach to this objective was to develop on the surface of fully densified silicon carbide (SiC) compatible surface structures which would distribute and reduce the point of impact shock loadings to which a SiC structural component might be subjected. Two methods were studied and evaluated; the chemical alteration of the SiC surface and the formation of porous layers on the SiC surface.

Attempts to chemically alter the surface of SiC by etching with fused salts resulted in the removal of intergranular material and thereby the formation of a thin, porous layer on the SiC. Porous layers of plasma-sprayed aluminum oxide and zirconium oxide were successfully applied to SiC surfaces. In each instance, however, it was necessary to grit-blast the SiC surface and precoat with nickel aluminide in order to achieve good adhesion of the oxide layer. Although fused salt etching produced a thin, porous layer of the surface of the SiC, serious degradation in strength also occurred. Strength values were also lowered by the processing steps employed to form adherent porous oxide layers on SiC surfaces.

A high-temperature Charpy impact test equipment was devised, using hydrogen-oxygen gas heating to bring the Charpy bar up to test temperature (1325°C). Rapid test determinations with good reproducibility were obtained with this innovation in test procedure.

A new approach to the formation of improved toughness in SiC high-temperature structural components equipped with an energy-absorbing layer (EAL) was discovered. It generated the concept that the ultimate component product could be fabricated in a one-step consolidation process. Further, it provided that SiC would be employed in the entire material system, with no added second-phase materials present. Problems associated with the presence of second materials, such as chemical interactions, differences in thermal expansion and bonding, would therefore be completely avoided. This approach featured the formation of a duplex pressureless sintered SiC body, the base of which is a fully sintered, dense, and strong SiC, and integrally bonded (sintered) to it, a porous SiC layer.

Results of microstructure studies, room temperature, and high temperature (1325°C) bend strength and impact tests are presented.

## II. INTRODUCTION

The successful utilization of brittle materials such as SiC and  $\text{Si}_3\text{N}_4$  in high-temperature turbomachinery will require materials and process developments which focus not only on the development of superior bulk properties and surface quality but also on improved toughness. One of the most restricting limitations to the broader application of SiC and  $\text{Si}_3\text{N}_4$  is that they are notably lacking in toughness, the ability to resist mechanical shock loading. The type of shock loading anticipated is that which arises during the collision of a foreign object traveling at high velocity with a ceramic structural component at rest relative to the foreign object. While the impact process is generally very complex, there are a few generalities that are observed when failure criteria can be established for the involved materials. For example, if a material can be defined to fail at a critical value of strain then it can be shown that local permanent set or local failure must necessarily occur at the point of contact if the ratio of impact velocity to sound velocity in one or another of the materials exceeds such a strain value. (The critical value of strain for a brittle material might be that at which local crack propagation occurs or for a plastically deformable material the critical strain might be that at the elastic limit.) Thus, if a plastically deformable material impacts with a brittle material, it is evident that the question of whether or not the brittle material sustains damage is an intimate function of the elastic strain limit of the impacting, plastically deformable material. A further case of importance is that of impact in which both bodies are of materials that are hard and brittle. It can be anticipated that such impacts could occur from the acceleration of small, hard particles in high temperature gas streams to velocities approaching Mach 1. At such speeds, the velocity ratios (particle velocity/sound velocity in the solid) for hard materials are of the order of  $10^{-3}$  to  $3 \times 10^{-4}$ . These values are in the range of fracture strains for brittle materials; thus if local damage on a large impacted structure is to be avoided, the sound velocity in the impacted structure should be substantially higher than that in the hard impacting particle.

Since the sound velocity of a material is a direct function of the Young's Modulus to density ratio for that material, then for both the above high velocity cases, the ability of a ceramic material to resist local impact damage is improved if this ratio is selected to be as high as possible. Such a choice is also consistent with the other desirable fact that the static strengths of ceramic materials are also a direct function of Young's Modulus.

There is a further and more important generality that may be observed from detailed considerations of the impact process. Momentum exchange and energy transfer occur only during the time in which the impacting bodies are physically in contact. Since momentum is the integral of the force-time product, it is evident that any mechanism that prolongs the contact time or increases the effective contact area between two impacting bodies will be

beneficial in reducing the maximum stresses generated at the point of impact. This is an important consideration in attempting to devise means whereby load-bearing structures are to be designed for improved resistance to local damage from impact loadings. For the more usual range of impact velocities, the duration of contact of impacting bodies varies, in general, as a direct function of the compliances and not of the moduli of materials. It is apparent, therefore, that adequate performance of a material under all types of loading requires, simultaneously, both high strength and high compliance. To a degree, and particularly for a single ceramic, these requirements are mutually inconsistent. For local failure, they point up the necessity of considering special materials preparation procedures in order to obtain acceptable trade-offs between these requirements.

A promising approach to the problem of improving the toughness of a high-strength refractory ceramic then, is to provide a surface that would:

- Absorb impact energy by both elastic and inelastic processes.
- Prolong the time of impact contact to decrease the maximum momentary loads imparted to the substrate material.
- Redistribute the applied load over a larger area, and thereby decrease the applied contact stress.

These surfaces could be non-load-bearing structures which are crushable or deformable and which are interposed between the load-bearing structure and the impacting body.

During the conduct of this investigation, the base values for Charpy impact strength and three-point bend strength of hot-pressed SiC were determined at both room temperature and at 1325°C. Charpy impact tests at 1325°C were made rapidly and with good reproducibility using a modified test machine and O<sub>2</sub>/H<sub>2</sub> gas torches for heating the specimen in place on the test machine.

Several techniques for applying porous layers on the hot-pressed SiC were evaluated, including:

1. Chemical etching of the SiC by fused salt treatment.
2. Fusion bonding of elemental silicon.
3. Plasma-spray-coated aluminum and zirconium oxides.

### III. MATERIALS, PROCEDURES, AND RESULTS

#### A. BASE MATERIALS

During the conduct of this program three different hot-pressed SiC ceramics were used. One of these was a hot-pressed ceramic product purchased from The Ceradyne Inc. and identified as Ceralloy 146A. The other two were hot-pressed at the General Electric Research and Development Center using SiC powders from two different sources and synthesized by completely different techniques. One class of the latter two powders was prepared by a General Electric proprietary process involving the reduction of a commercially available silica. These were designated as IHP powders or ceramics. The second class of powders used were made by the Pittsburgh Plate Glass Company using gas phase reactions involving  $\text{SiCl}_4$  and certain hydrocarbons.

##### 1. Ceralloy 146A

A representative sample of Ceralloy 146A hot-pressed ceramic was microscopically examined to establish a baseline character of its microstructure. Figure 1 suggests the material contained a small amount of porosity, probably less than 2 v/o. When the same specimen was thermal etched at 1550°C in argon for 20 minutes, the microstructure revealed in Figures 2 and 3 was noted. A uniform grain size of between 15 and 20  $\mu\text{m}$  can be measured. Figure 3 was interesting in that it revealed a second phase material which had to a degree become molten during the thermal etching treatment. Microprobe analyses of other silicon-rich SiC materials suggests that this second phase material was also a silicon-rich melt. As indicated by bend strength measurements shown in Table I, the microstructural character of the Ceralloy 146A suggested that at temperatures below which the intergranular second phase material will begin to yield under stress, the structural integrity was considered to be quite good.

Three-point bend test bars (5.08 mm x 2.54 mm x 4.45 cm) made from Lot A Ceralloy 146A and fracture strengths at room temperature and at 1325°C were determined. Tests were conducted using a crosshead speed of  $5 \times 10^{-3}$  cm/minute for the room temperature tests and  $12.7 \times 10^{-3}$  cm/minute at 1325°C. The results of these tests are summarized in Table I. Although the crosshead speeds employed for the two-temperature tests were not the same, very little difference in the resulting strength measurements would be expected.

As can be readily noted there was a serious degradation in the room temperature bend strength, when measured at the test temperature of 1325°C. This can most likely be related to the presence and high temperature creep character of the second phase material revealed in the SEM photomicrograph (Figure 3).

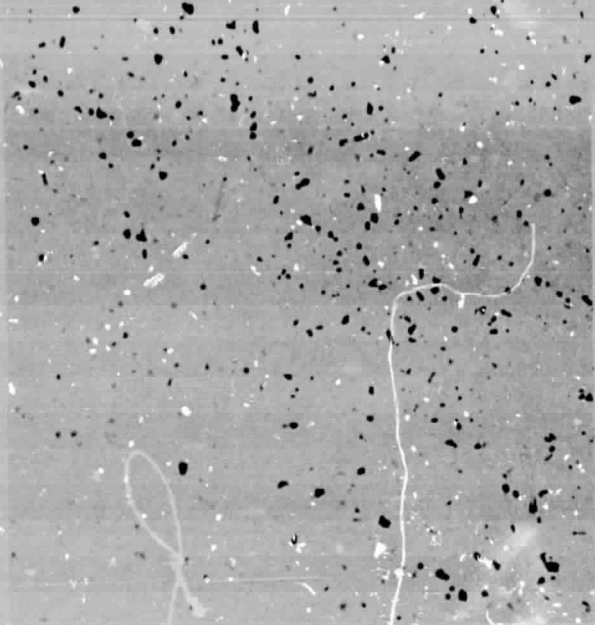


Figure 1. Ceramloy 146A SiC - Polished 263X

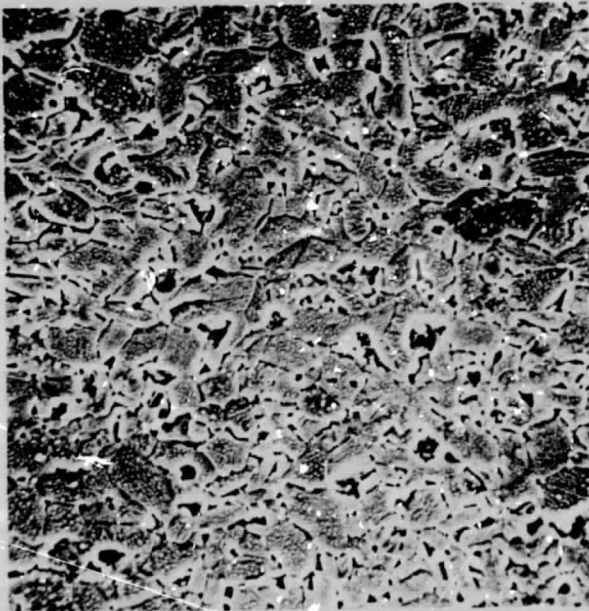


Figure 2. SEM Photomicrograph of Ceramloy 146A SiC - Polished and Thermal Etched at 1550°C for 20 minutes in Argon 500X

ORIGINAL PAGE IS  
OF POOR QUALITY

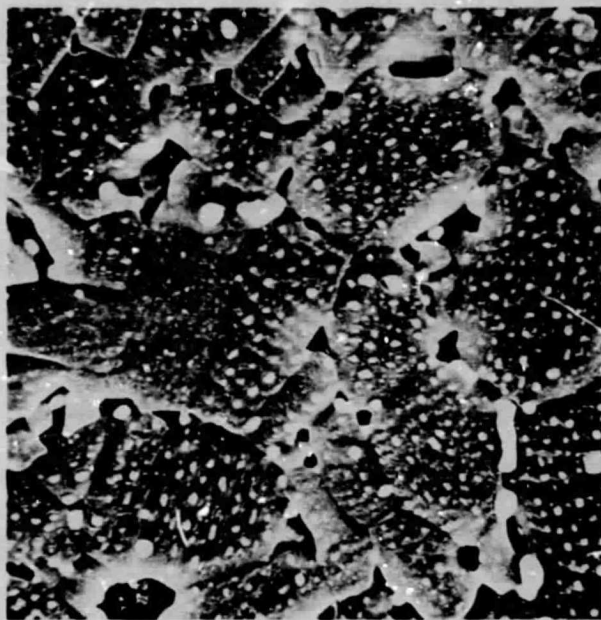


Figure 3. SEM Photomicrograph of Cer alloy 146A SiC - Polished and Thermal Etched at 1550°C for 20 minutes in Argon  
2000X

Table I  
THREE-POINT BEND TEST FRACTURE STRENGTHS  
OF CERALLOY 146A  
(Bend Test Bars 5.08 mm x 2.54 mm x 4.45 cm)

Sample Identification	Fracture Load (Kg)	Room Temperature Fracture Strength (MN/m <sup>2</sup> )	Fracture Strength at 1325°C (MN/m <sup>2</sup> )
D 1287	31.5	536	-
D 1288	30.3	519	-
D 1289	28.2	487	-
C 9085	16.4	-	277
C 9086	13.6	-	231
C 9087	14.1	-	239
C 9088	15.9	-	271
C 9089	13.1	-	223
Average value of fracture strength		(514)	(248)

Eight standard sized impact test bars (6.35 mm x 6.35 mm x 5.08 cm) were fabricated and room temperature impact strength determined on the as-ground specimens. A Manlabs Charpy Impact test machine, Model CIM-24 was used in these early determinations of base-line impact strength. This test machine was set up to accept a specimen with a 3.97 cm unsupported span. The impact test results on 8 specimens of Ceralloy 146A run at room temperature are shown in Table II.

Table II  
IMPACT STRENGTH OF CERALLOY 146A

Sample No.	Impact Strength (Joules)
1	0.32
2	0.14
3	0.15
4	0.13
5	0.19
6	0.16
7	0.23
8	0.14
(average value of 8)	(0.18)

All of the specimens fractured close to their mid-points, indicating that there were no gross internal flaws, voids, or imperfections in the samples. Surface roughness and linear grain size measurements were made on three of the eight Charpy impact test bars in an attempt to identify any structural differences which might account for the difference in the observed impact strengths. Surface roughness was measured on two faces of the test bar, one against the anvil and the opposite one facing the hammer. A Dek-TaC precision profilometer made by Sloan was used. The fracture surfaces of the test bars were polished and etched and linear grain size measurements were made. The results of these examinations are shown in Table III.

No great differences in structure, grain size or surface roughness could be observed in the #1 and #8 samples. Sample #4, however, appeared to have some areas in the fracture surface which varied in density. This feature may account for it having the lowest impact strength of the eight specimens tested.

Table III  
SURFACE PROFILE AND GRAIN SIZE MEASUREMENTS  
OF CERALLOY 146A

Charpy Impact Test Bar No.	Charpy Impact Strength (Joules)	Surface Profile ( $\mu\text{m}$ )	Average Grain Size at Fracture Surface ( $\mu\text{m}$ )
1	0.32	0.4 (range 0.2-0.8)	7
4	0.13	0.6 (range 0.2-1.1)	8
8	0.14	0.3 (range 0.1-1.1)	7

## 2. Hot-Pressed Powder (GE-IHP Series and PPG -- #JP49)

A number of hot pressings of 7.62 cm diameter SiC discs, 1.27 cm to 1.91 cm thick, were made using powders and consolidation procedures developed within this laboratory. Satisfactory densities were achieved with pressings at 2000°C and 1900°C; however, an unsatisfactory degree of exaggerated grain growth was experienced in those billets prepared at these temperatures. Subsequent pressing at 1820°C of powders, prepared by silica reduction, yielded a fine-grained ceramic without exaggerated grains. A Pittsburgh Plate Glass SiC powder prepared to our specifications regarding boron and carbon dopants, was also consolidated by hot pressing. This latter material pressed at 1820°C (hot press run #JP49) was found to contain a small amount of secondary grains. The amount of this exaggerated grain growth was, however, considerably less than that found in the samples initially pressed at 1900°C and 2000°C.

Table IV gives a summary of the experiments made to identify the conditions required to achieve the desired microstructure and avoid the large grain structure which leads to degradation in mechanical properties.

Figures 4 through 10 show the improvement in microstructure achieved by lowering the temperature of hot pressing from 2000°C to 1820°C. Although no significant loss in final density occurred in the 1.91 cm thick specimens when pressed at 2000° and 1820°C, it should be noted that a loss of 2% in density did result. The massive amount of exaggerated grain growth occurring at 2000° and 1900°C hot-pressing temperatures is clearly evident in Figures 4, 5, and 6. Figure 7 shows the 40 to 50 micron needles formed during the hot pressing at 1820°C of the purchased SiC powder. Figures 8, 9, and 10 show the fine-grain microstructure developed in hot-pressed discs made from internally synthesized and formulated SiC powders.

Table IV  
HOT-PRESSED SiC RUNS

Hot-Press Run #	SiC Powder Identification	Size of Pressing dia./thick (cm)	Hot-Pressing Conditions °C/MN/m²/min	Density g/cc	Microstructure Character
IHP1A	GE with 2% BN + 0.5% B + 0.7% C	7.62/1.91	2000/41.4/30	3.17	Large, prismatic grains, 300-500 $\mu$
IHP2	GE with 1% B + 0.7% C	7.62/1.91	2000/41.4/30	3.18	Large, prismatic grains, 500 $\mu$
IHP1A-2	GE with 2% BN + 0.5% B + 0.7% C	7.62/1.91	1900/41.4/50	3.17	Very large, prismatic grains, 10,000 $\mu$
JP #49	PPG Powder (GE Specs.)	7.62/1.27	1820/41.4/50	3.17	Needle-like grains 50 $\mu$
IHP3	GE with 2% BN + 0.5% B + 0.7% C	7.62/1.27	1820/41.4/50	3.14	Fine-grain structure 7 $\mu$
IHP3-A	GE with 2% BN + 0.5% B + 0.7% C	7.62/1.27	1820/41.4/50	3.16	Fine-grain structure 6 $\mu$
IHP3-B	GE with 2% BN + 0.5% B + 0.7% C	7.62/1.91	1820/41.4/50	3.11	Fine-grain structure 6 $\mu$



Figure 4. Specimen No. IHP1A Thermal-etched at 1500°C -  
(1 mm = 16.6  $\mu$ m)

60X

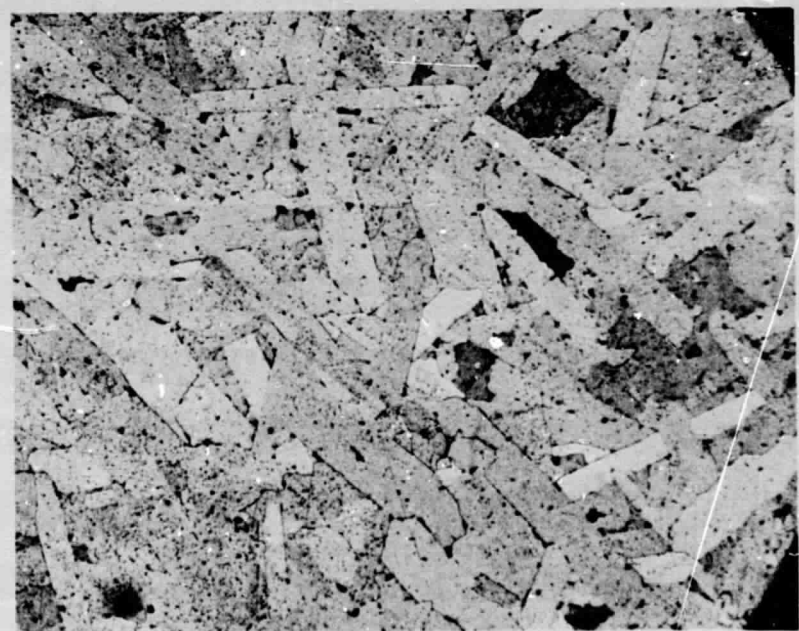


Figure 5. Specimen No. IHP2 Thermal-  
etched at 1500°C - (1 mm =  
15  $\mu\text{m}$ ) 66X

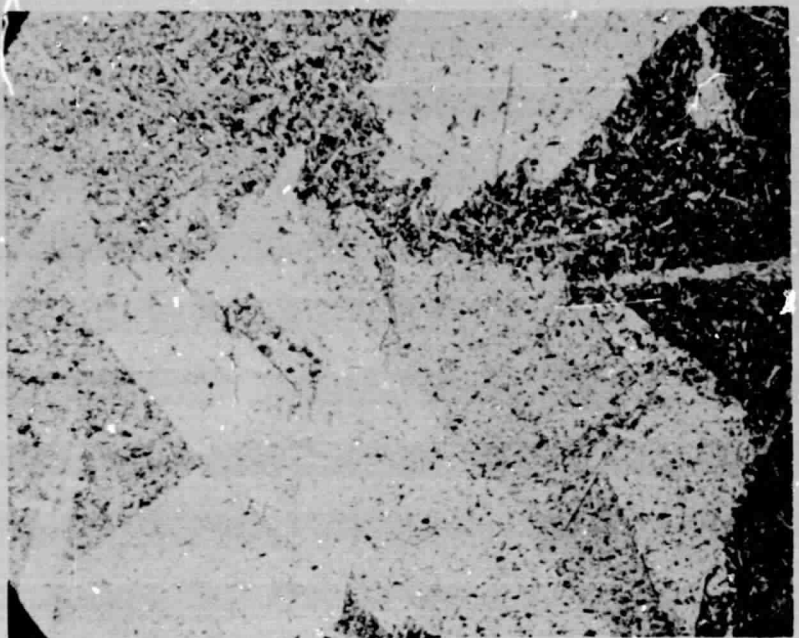


Figure 6. Specimen No. IHP1A-2 Thermal-  
etched at 1500°C - (1 mm =  
15  $\mu\text{m}$ ) 263X

ORIGINAL PAGE IS  
OF POOR QUALITY

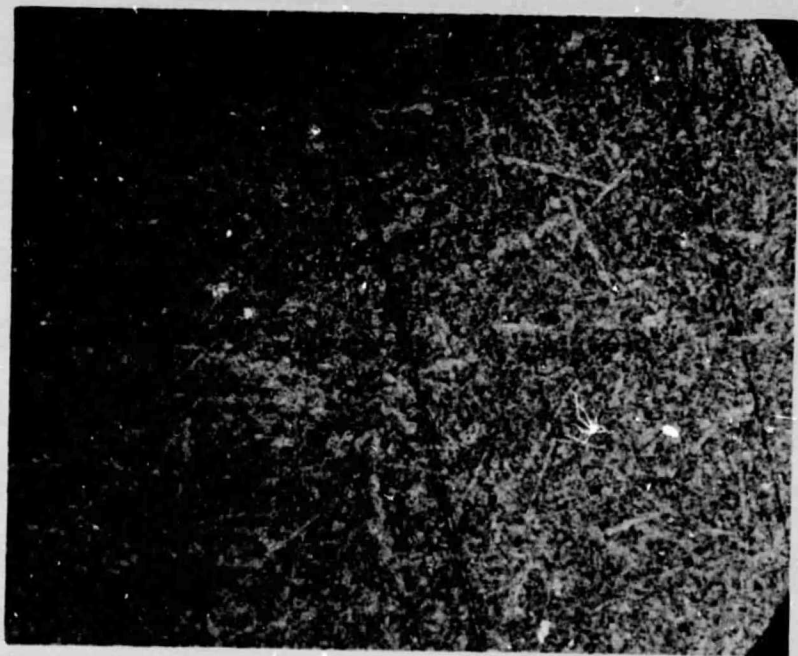


Figure 7. Specimen No. JP #49 Thermal-  
etched at 1500°C - (1 mm =  
3.8  $\mu$ m)  
263X

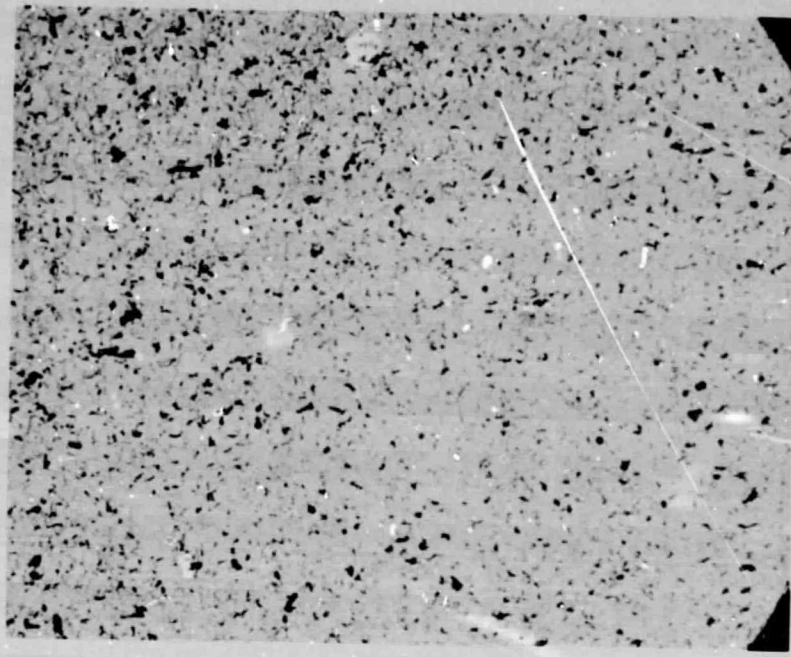


Figure 8. Specimen No. IHP3 Thermal-  
etched at 1500°C - (1 mm =  
3.8  $\mu$ m)  
263X

ORIGINAL PAGE IS  
OF POOR QUALITY

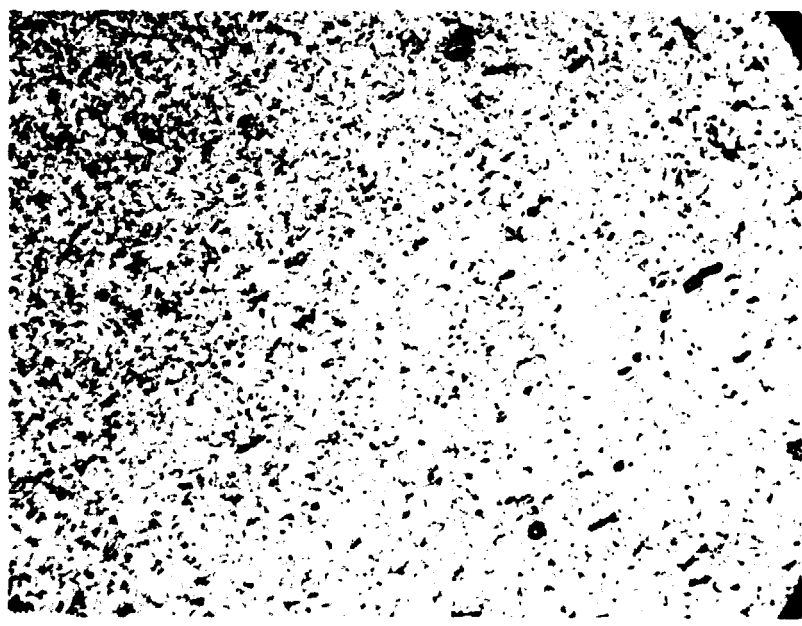


Figure 9. Specimen No. IHP3-A Thermal-  
etched at 1500°C - (1 mm =  
3.8  $\mu$ m) 263X

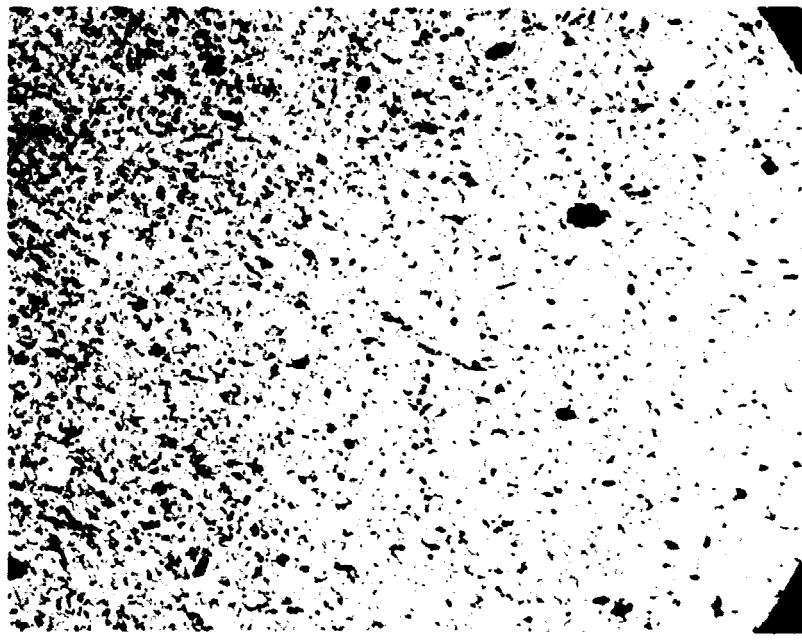


Figure 10. Specimen No. IHP3-B Thermal-  
etched at 1500°C - (1 mm =  
3.8  $\mu$ m) 263X

Although it was recognized that because of the large grains present in specimens IHP1A and IHP2, the mechanical properties would be poor and there would be considerable scatter in the results. It was decided to perform Charpy impact tests both at room temperature and at 1325°C using a 1.356 to 2.712 J Charpy test unit. The results are shown in Table V. The tests were performed on unnotched 6.35 mm square x 5.08 cm long Charpy bars using the 1.356 J hammer on the test machine.

Table V  
CHARPY IMPACT TESTS ON IHP1A and IHP2 HOT-PRESSED SiC

IHP1A		IHP2	
Room Temperature Impact Strength (Joules)	1325°C Impact Strength (Joules)	Room Temperature Impact Strength (Joules)	1325°C Impact Strength (Joules)
0.373	0.164	0.057	0.057
0.084	0.231	0.063	0.057
0.035	0.401	0.070	0.063
0.316	0.226	0.042	0.050
0.305	0.078	0.060	0.052
<u>0.070</u>	<u>0.066</u>	<u>0.063</u>	<u>0.060</u>
Ave. 0.198	0.194	0.060	0.057

As is readily noted, sample IHP1A exhibited extreme variation in impact strength at both room temperature and 1325°C. Although it is only one-third as strong in impact as the average of IHP1A, sample IHP2 exhibited remarkably good consistency in results and with little sensitivity to temperature. It was considered to be of little, if any, value to go any further with the mechanical properties of these specimens. Consequently, fracture strengths were not determined. Additionally, no mechanical properties were determined on IHP1A-2, also because of the excessively large amount of grain growth occurring in this specimen.

Three-point bend test fracture strengths were determined at room temperature and at 1325°C on specimen run numbers JP #49, IHP3, IHP3A, and IHP3B. Test bar configuration was nominally 5.08 mm wide x 2.54 mm deep x 5.08 cm long. In the test equipment, the unsupported length was 3.81 cm. The surfaces of the test bars were "as-ground" having profiles averaging close to 0.5  $\mu\text{m}$ . Before fracture tests were made, each test bar was examined for edge flaws. When present, the edges were smoothed with a 600 grit diamond hone, while observing the work under a low-power microscope.

Table VI

**THREE-POINT BEND TESTS ON HOT-PRESSED SiC**  
**(Test Bars Nominally 5.08 mm x 2.54 mm x 3.81 cm Span)**

Hot-Press Run No.	Specimen No.	Room Temperature Fracture Strength (MN/m <sup>2</sup> )	Specimen No.	1325°C Fracture Strength (MN/m <sup>2</sup> )
JP #49	D-1411	353	C-9397	415
	D-1412	378	C-9398	425
	D-1413	463	C-9399	383
	D-1414	392	C-9400	478
	Average JP #49	397		425
IHP3	D-1407	419	C-9393	449
	D-1408	343	C-9394	480
	D-1409	506	C-9395	541
	D-1410	539	C-9396	446
	Average IHP3	452		479
IHP3-A	D-1415	477	C-9431	422
	D-1416	474	C-9432	454
	D-1417	362	C-9433	499
	Average IHP3-A	438	C-9433	458
IHP3-B	D-1418	525	C-9434	421
	D-1419	476	C-9435	461
	D-1420	342	C-9436	348
	Average IHP3-B	448		410

The individual test results are shown in Table VI along with the average value for each group. Significant features in these data include the apparent increase in bend strength from room temperature to 1325°C. However, IHP3-B was different in this regard. It suffered about an 8% loss in strength when tested at 1325°C as compared to a 6% gain for JP #49, IHP3, and IHP3-A. One apparent difference in strength-sensitive character is the lower density of the IHP3-B material. The additional porosity in this specimen may be responsible for its lower high temperature strength. Further examination of the data revealed the apparent degrading effect on the bend strengths at both room temperature and at 1325°C of the small amount of needle-like growth in JP #49 as opposed to the fine-grained structure developed in IHP3 and IHP3-A.

Charpy impact tests were completed on two of the four hot-pressed SiC specimens. These tests employed unnotched bars nominally 6.35 mm x 6.35 mm x 3.81 cm (span) in size and a 1.356 J hammer. The test results are shown in Table VII.

Table VII

CHARPY IMPACT TESTS ON HOT-PRESSED SiC SPECIMENS  
JP #49 and IHP3  
(Test Bars Nominally 6.35 mm x 6.35 mm x 3.81 cm Span)

Hot-Press Run No.	Specimen No.	Room Temperature Impact Strength (Joules)	Specimen No.	1325°C Impact Strength (Joules)
JP #49	A	0.266	D	0.402
	B	0.289	E	0.471
	C	0.262	F	0.375
Average JP #49				0.416
IHP3	1/A	0.334	4/D	0.355
	2/B	0.376	5/E	0.361
	3/C	0.445	6/F	0.382
Average IHP3				0.366

The Charpy impact strength tests indicated excellent reproducibility of the test conditions. Again, the needle-like grain growth occurring in JP #49 may account for its room temperature impact strength being lower by about 30% of the value obtained for the comparison billet IHP3.

Although there was little change in the average 1325°C Charpy impact strength for IHP3, it was about 5% lower than the room temperature value. Most interesting of all was the more than 50% increase in average Charpy impact strength that occurred at 1325°C for the JP #49 specimen as compared to its room temperature impact strength. This appeared to be a real effect in view of the fact that the individual percentage increases for all three specimens of JP #49 tested underwent increases ranging from 43% for specimen C to 63% for specimen B. Specimen A fell in between with an increase of 51%. No complete explanation can be given at this time for this behavior in the JP #49 specimen. One might expect, on the basis that the impact strength will increase as the square of the fracture bend strength, to note perhaps a 15% corresponding increase in impact strength at 1325°C from the room temperature value. Observed increases, however, of 3 to 4 times this amount require additional explanation.

Table VIII gives a summary of the averaged values of bend and Charpy impact strength in hot-press runs JP #49 and IHP3.

**Table VIII**  
**SUMMARY OF AVERAGE VALUES OF BEND AND CHARPY IMPACT  
 STRENGTHS OF HOT-PRESSED SiC SPECIMENS JP #49 and IHP3**

Hot-Press Run No.	Room Temperature Bend Strength (MN/m <sup>2</sup> )	1325°C Bend Strength (MN/m <sup>2</sup> )	Room Temperature Charpy Impact Strength (Joules)	Room Temperature Charpy Impact Strength (Joules)
JP #49	397	425	0.272	0.416
IHP3	452	479	0.385	0.366

The fracture surfaces of Charpy test specimens No. D (JP #49) and 4/D (IHP3), both of which were determinations of impact strength at 1325°C, were examined by electron microscopy at 6000X. The electron micrographs taken of these surfaces are shown in Figures 11 and 12. They clearly show that high temperature fracture occurred transgranularly in both materials. In addition, they reveal what appears to be some internal cracks. It is difficult to say at this time how the cracks were generated in the first place. They may have formed in the hot-pressing stage. They may be thermal stress cracks occurring during the heat-up to 1325°C stage for the Charpy tes . A third possible explanation would be that they developed at the time of impact in the Charpy test and were stopped further along the length of the test bar. It seems likely that the last explanation would be most valid.



**Figure 11. Fracture Surface, Test Specimen No. D (Hot-press JP #49)  
 Charpy Impact Test at 1325°C - (1 cm = 3.03 μm) 3300X**

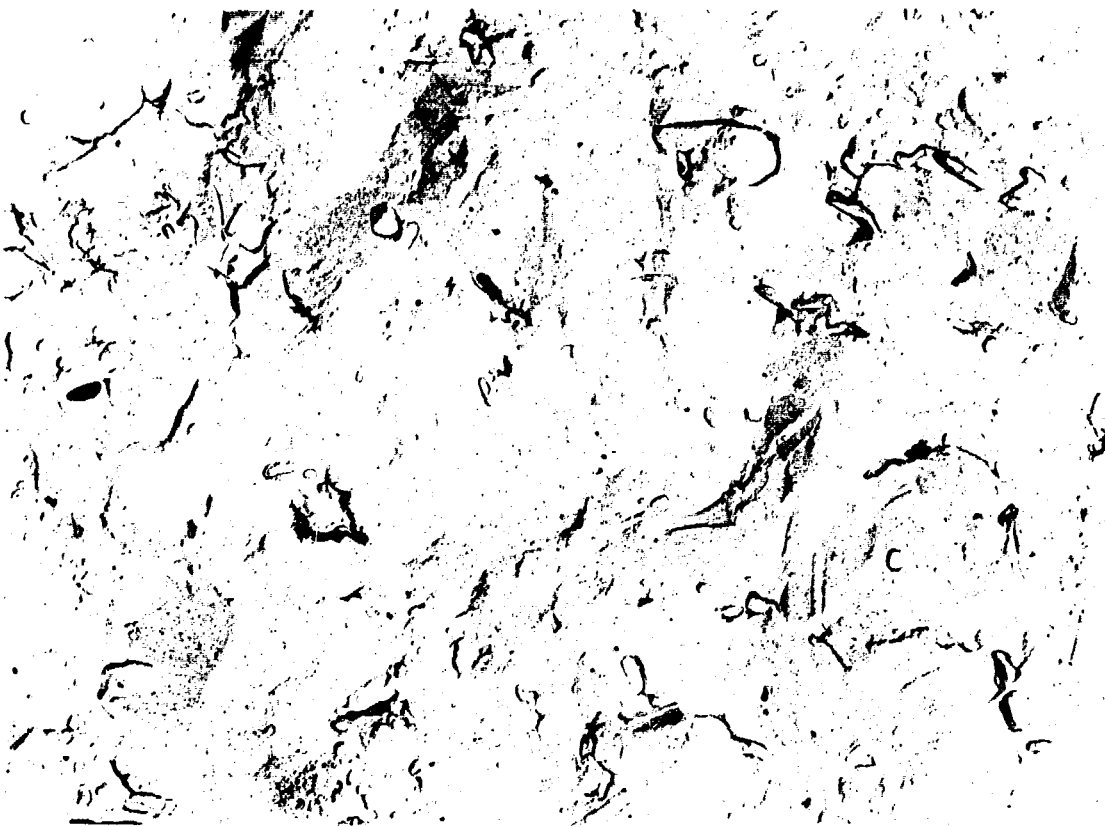


Figure 12. Fracture Surface, Test Specimen No. 4/D (Hot-press IHP3)  
Charpy Impact Test at 1325°C - (1 cm = 2.44 μm) 4100X

Charpy impact tests were also run on IHP3-A and IHP3-B. Standard test bars were machined from the hot-pressed billets and impacted with a 1.356 J hammer. Test results were obtained at both room temperature and at 1325°C, as shown in Table IX.

Table IX  
CHARPY IMPACT TESTS ON HOT-PRESSED  
SiC SPECIMENS IHP3-A AND IHP3-B  
(Test Bars Nominally 6.35 mm × 6.35 mm × 3.81 cm Span)

Hot-Press Run No.	Specimen No.	Room Temperature Impact Strength (Joules)	Specimen No.	1325°C Impact Strength (Joules)
IHP-3A	1	0.197	3	0.199
	2	0.048	4	0.194
	-	-	5	0.183
IHP-3B	6	0.148	9	0.096
	7	0.199	10	0.202
	8	0.165	11	0.179

If the two less-than-unity impact strength values are not considered, the consistency of the values was relatively good. However, most disturbing was the fact that the generally indicated value for both room temperature and 1325° C impact strength of about 0.192J was, just about half of the value obtained for billet IHP3 (see Table VII). It was reasonable to expect that the impact strength values for billets IHP3, IHP3-A, and IHP3-B would be very close to one another, since each of the 3 billets was made with the same powder. Likewise, processing conditions were the same in each of the three hot-pressings.

During the course of trying to find an explanation for the discrepancy noted, it was learned that a high density alumina insulating brick had been used as a backing in the test equipment during the Charpy determinations for IHP3-A and IHP3-B. A lower density alumina backing had been used for the tests on JP #49 and IHP3. It was thought then that the discrepancy could be explained by the position that impact strengths for JP #49 and IHP3 were determined on a "more compliant" machine than the runs for IHP3-A and IHP3-B.

To determine the effect, if any, of the backing material on the Charpy test results, carefully machined Charpy test bars of Plexiglas were made and tested at room temperature with three different backings.

1. The insulating alumina ( $\rho=1.4$  gm/cc) system used for the tests on JP #49 and IHP3.
2. The insulating alumina ( $\rho=2.5$  gm/cc) system used for the tests on IHP3-A and IHP3-B.
3. Steel anvils.

Ten to fifteen bars were impact-tested with each of the three backing materials. The average impact strength values for the Plexiglas bars on the two insulating alumina backing systems were the same, namely 0.407 J. With the steel anvils, the average impact strength of the Plexiglas bars was 0.350 J.

Since no differences in impact strength were noted for the Plexiglas bars using the two alumina systems, a difference in machine compliance did not explain the discrepancy in the values determined on SiC. Neither did a review of the test data and impact test procedures used, disclose any accountable reasons for the differences noted.

## B. ENERGY-ABSORBING LAYERS (EAL's)

### 1. Molten Salt Etch

One approach employed to chemically form a porous layer on hot-pressed SiC was to treat the SiC with a molten salt bath. This was done with 6 bend

test bars of Ceralloy 146A (Lot A). The specimens were exposed for 30 minutes in a molten bath of the following composition, at a temperature of 830°C:

$\text{CaCl}_2$  - 72 w%

$\text{CaF}_2$  - 18 w%

$\text{CaSO}_4$  - 10 w%

Figures 13 and 14 are SEM photomicrographs of the as-treated SiC surface at 500X and 2000X, respectively. They indicate that a uniform surface structure had been created which had no visible intergranular bond. The fact that it was an abrasion-resistant surface, however, also indicated that the grains were indeed bonded below the visible surfaces.



Figure 13. SEM Photomicrograph of Ceralloy 146A SiC - Treated in a  $\text{CaCl}_2\text{-CaF}_2\text{-CaSO}_4$  molten salt bath at 830°C for 30 minutes.  
500X

Bend strength tests were made at room temperature and at 1325°C on the molten salt-treated specimens. The results of these tests are shown in Table X.

The results of these tests indicated that a considerable degradation in bend strength resulted from the molten salt treatment.

Room temperature Charpy impact tests were conducted on Ceradyne's hot-pressed SiC, identified as Ceralloy 146A, and which had been fused-salt-treated, as described above. These tests were run on a Manlabs



Figure 14. SEM Photomicrograph of Ceralloy 146A SiC - Treated in a  $\text{CaCl}_2$ - $\text{CaF}_2$ - $\text{CaSO}_4$  molten salt bath at  $830^\circ\text{C}$  for 30 minutes. 2000X

Table X

THREE-POINT BEND TEST FRACTURE STRENGTHS  
OF CERALLOY 146A AFTER TREATMENT  
IN  $\text{CaCl}_2$ - $\text{CaF}_2$ - $\text{CaSO}_4$  MOLTEN SALT BATH

Sample Identification	Fracture Load (Kg)	Room Temperature Fracture Strength (MN/m <sup>2</sup> )	Fracture Strength at $1325^\circ\text{C}$ (MN/m <sup>2</sup> )
D 1290	19.9	346	-
D 1291	18.6	340	-
D 1292	20.2	351	-
C 9090	7.3	-	126
C 9091	6.3	-	107
C 9092	5.6	-	100
Average values of fracture strength		(346)	(110)

Charpy impact tester, Model No. CIM-24. Serious degradation of impact strength from the baseline average value of 0.183 J, occurred as a result of this treatment. In three tests, values of 0.093, 0.097, and 0.085 Joules were determined, indicating good reproducibility to the surface treatment and impact test procedures, but disappointingly low values.

These data confirmed the expectations that there would be a serious degradation in impact strength at the time we completed the three-point bend tests on the unetched and etched specimens of the Ceralloy 146A. The fracture strengths at room temperature were 514 MN/m<sup>2</sup> for the unetched specimens and 346 MN/m<sup>2</sup> for the etched samples, a 33% reduction in fracture strength due to the etch treatment. At that time, we expected the Charpy impact strength would be reduced by about 50% due to the P<sup>2</sup> (P = load to fracture) term in the energy of impact relationship

$$E = \frac{P^2 t^3}{8Ebh^3}$$

Having made these determinations on the fused salt etch approach, it appeared that further work in this direction would not prove fruitful and that approach was terminated.

## 2. Porous Si<sub>3</sub>N<sub>4</sub> on SiC

This approach consisted of applying a fused silicon film to the surface of silicon carbide and reaction-sintering the silicon in a nitriding atmosphere to produce a porous adherent Si<sub>3</sub>N<sub>4</sub> layer on the denser substrate ceramic.

200 Silicon powder, Cat. No. S-164, from the Fisher Scientific Co., was mixed with a solution of ethyl cellulose in amyl acetate and painted on silicon carbide test bars. After evaporation of the amyl acetate, a layer of silicon particles bonded together and to the substrate by the ethyl cellulose remained on the test bar. Removal of the ethyl cellulose was accomplished by pyrolytic decomposition between 1430° and 1475°C. Binder removal was attempted in three different atmospheres: nitrogen, argon, and vacuum. Heating and cooling rates were each 20 minutes long with soak times at temperature of 5 to 30 minutes. Initial results indicated that extremely careful control of atmosphere purity was necessary to prevent oxidation of the silicon during processing. Oxidation to varying degrees occurred in all three atmosphere conditions that were used. In those cases where oxidation was severe, the silicon would not bond to the SiC nor to itself. Where oxidation of the Si was less severe, it apparently formed a good but uneven bond to the SiC substrate. Figure 15 shows the islands of fusion-bonded silicon to silicon carbide. Since the desired and final layer of Si<sub>3</sub>N<sub>4</sub> was required to be both porous and evenly distributed over the surface of the SiC, this approach to that end did not appear to be too promising. The uneven wetting of the SiC by Si was not desirable. Because of this situation, further work was not expected to be worthwhile, and this approach was also terminated.



Figure 15. Elemental Si Fusion - Bonded to SiC Substrate 15X

### 3. Porous Alumina on SiC

Plasma-sprayed layers of  $\text{Al}_2\text{O}_3$  applied directly to a SiC surface lacked sufficient adhesion to function as an energy absorption layer. Figure 16 shows plasma-sprayed alumina directly applied onto SiC pulled away from the substrate.

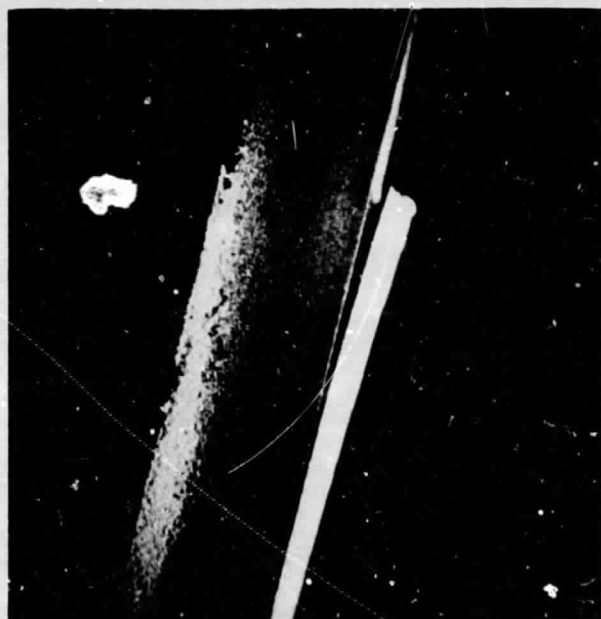


Figure 16. Plasma-sprayed  $\text{Al}_2\text{O}_3$  Directly Applied onto SiC Ceramic. 8X

In order to provide a material system in which the energy-absorbing layer would adhere to the SiC surface, it was necessary to lightly grit-blast the SiC test piece. The grit-blast surfacing of the SiC resulted in a reduction of the room temperature bend strength of the Ceralloy 146A from the previously determined average value of 513 MN/m<sup>2</sup> to 455 MN/m<sup>2</sup>, a reduction of 11%. All the grit-blasted test bars were first plasma-sprayed with 0.025 mm of a NiAl/Ni<sub>3</sub>Al composition, which was also required in order to provide adhesion of the oxide layer to follow. Following the nickel aluminide surfacing, a series of test bars were prepared with 0.127 mm of Al<sub>2</sub>O<sub>3</sub>, 0.254 mm and 0.381 mm layers of ZrO<sub>2</sub>. Layers of Al<sub>2</sub>O<sub>3</sub> thicker than 0.127 mm did not adhere, spalling off the substrate soon after application. The EAL was applied to only one of the 5.08 mm × 2.54 mm × 4.45 cm surfaces of the test bar. Bend tests were then made with the EAL on the compression side of the bar at room temperature and at 1325°C.

In order to obtain some indication as to the effect on impact strength of the surface treatment and plasma-sprayed oxide layers, room temperature Charpy tests were conducted on these material systems using bend test bars as specimens. It was felt that any differences in impact strength due to the EAL could be noted, and if warranted, additional determinations would be made.

The results of the three-point fracture-strength tests and the Charpy impact tests on the plasma-spray coated specimens are summarized in Table XI.

Table XI  
SUMMARY OF FRACTURE STRENGTH AND IMPACT STRENGTH  
OF PLASMA-SPRAY COATED SiC SPECIMENS

Specimen Surface Treatment	Average R. T. Fracture Strength	Average 1325°C Fracture Strength	Average R. T. Impact Strength (Non-Standard** Charpy Bar)
As-machined	514 MN/m <sup>2</sup>	248 MN/m <sup>2</sup>	--
Grit-blasted	456	--	0.046 Joules
0.127 mm Al <sub>2</sub> O <sub>3</sub> / 0.025 mm NiAl	354*	214*	0.025
0.254 mm ZrO <sub>2</sub> / 0.025 mm NiAl	334*	166*	0.029
0.381 mm ZrO <sub>2</sub> / 0.025 mm NiAl	351*	145*	0.034

\* EAL in compression

\*\*5.08 mm × 2.54 mm × 4.45 cm

In addition, one set of three specimens having an 0.254 mm EAL of  $\text{ZrO}_2$  were bend-tested at room temperature with the EAL on the tensile side of the specimen as it was broken. The average value of these three tests was 266 MN/m<sup>2</sup>, a 20% reduction.

It was noted that the total effect of processing to apply an EAL by plasma-spraying resulted in serious degradation of the fracture strength of the substrate SiC. The room temperature tests showed that the net effect on fracture strength of grit-blasting the SiC surface, application of plasma-sprayed nickel aluminide, and application of plasma-sprayed oxide layers lowered the fracture strength of the SiC from about 511 MN/m<sup>2</sup> to about 345 MN/m<sup>2</sup> a reduction in strength of some 32%. It was also noted that in the range of thickness examined that there was no effect on the room temperature fracture strength due to thickness of this type of EAL. All three values were close to 345 MN/m<sup>2</sup> for the three thicknesses of EAL tested.

The high temperature fracture data showed that there was an increasing degradation in fracture strength with increasing thickness of the plasma-sprayed EAL. For the 0.127 mm, 0.254 mm and 0.381 mm thick EALs, there were reductions in strength at temperature of 13.5%, 33.0%, and 41.5% respectively. This suggested a correspondence with time of exposure to temperature and plasma-spraying. Additionally, it suggested that there may be some chemical reaction between the SiC substrate and the nickel aluminide and/or oxide layers.

The room temperature impact data (on non-standard bars) also indicated that there was a general reduction in impact strength due to surface treatment and plasma-spraying. However, the values of impact strength for the 0.127 mm, 0.254 mm, and 0.381 mm thick coatings suggest that there may be some improvement in impact strength as the thickness of an EAL increases. The differences noted in these data are probably within the scatter band involved and no definite conclusions should be made in this regard.

As was found in the case of the fused-salt etch approach, it appeared that the processing steps required to obtain plasma-sprayed coatings of oxides on SiC degrade its mechanical strength to such a degree that the application of potential EALs onto SiC by plasma-spraying is not a viable approach to the objective.

Other techniques for applying an EAL to a SiC substrate were examined. It had been noted in other investigations that aluminum stearate added as a lubricant for die pressing SiC powders also appeared to have a beneficial effect on the self-bonding properties of the SiC powder. Preliminary experiments were made to determine if porous SiC and  $\text{Si}_3\text{N}_4$  layers could be prepared and bonded to SiC ceramic surfaces so as to function as a possible EAL. In both instances, organic vehicle slurries of SiC and  $\text{Si}_3\text{N}_4$  powders with aluminum stearate dissolved in the liquid organic vehicle were applied

by brushing onto SiC ceramic surfaces. These were dried and fired in N<sub>2</sub> at about 2000°C. Self-bonding of both compositions did occur, accompanied however, by only a partial degree of adhesion of the mixture to the SiC ceramic. Another approach to the formation of an EAL to the SiC surface which was explored was to fuse a glassy surface onto the ceramic. Of three high-temperature glasses examined, two were found to be non-wetting of the SiC surface and full of bubbles. The third, a General Electric glass, #1462, also called "A" glass, was fused onto the SiC at 1500°C. It exhibited reasonably good wetting and bonding to the SiC. On cooling, however, it cracked but did not spall away from the SiC substrate.

### C. New Approach

The approaches examined to date to improve impact resistance by the formation of energy-absorbing layers of a variety of forms on fully densified SiC have not met with notable functional success. It was determined that a dense, strong SiC ceramic can be overlayed with a second material composition. It was also determined that it is generally necessary to etch or otherwise alter the surface profile of the SiC in order to obtain good adhesion of the overlay material. It was shown that such changes in the SiC surface apparently results in sufficient damage to the SiC surface that it causes serious degradation in the strength of the SiC.

It has been shown in the fused-salt etch approach in which, although there was a small degree of porosity created in the SiC surface to form what was hoped to be an EAL, that there was evidently sufficient damage caused to the surface of the SiC to result in strength values of only about 50% of those obtained on the unetched specimens. In order to obtain good adhesion of the plasma-sprayed EALs, it was necessary to first grit blast the SiC surface. Here, too, strength values were drastically lowered, due apparently to the surface damage created by the grit-blasting step. In the other approaches, too, including controlled oxidation of the SiC surface to produce SiO<sub>2</sub> layers, and the formation of glassy EALs on the SiC, similar observations were made.

In spite of the results obtained to date to improve impact resistance by the formation of energy-absorbing layers on fully dense SiC, it still remains a promising objective. Several benefits would accrue with the successful development of this approach.

- Preservation of the strength of a high-strength substrate by protection against handling damage and local damage under operating conditions.
- Preservation of the strength of the substrate by protection against machining damage. In this context, it is perfectly feasible that final machining to high tolerances of a part could be performed only on the easily machined coating material. Such machining would be rapid

and simple and prevent the initiation and propagation of damage cracks into the high strength substrate.

- Porous materials exhibit relatively low thermal conductivities and generally high resistance to thermal shock. They can therefore act as a thermal barrier to reduce temperature gradients in a substrate material and thus improve the apparent mechanical performance of that material.
- Porous coatings provide resistance to and distribute contact stresses that originate in the grips and attachments necessary to fasten a ceramic part to any other machine part. This attachment problem is one of the most severe problems faced by the turbo-machinery designer. Its solution will require specific attention to surface modification processes.
- Particularly for glancing, small particle impact, porous coatings provide an energy absorbing mechanism to prevent local damage to strong, substrate materials.

To achieve the benefits from coating procedures, the coating itself is subject to many constraints relative to the substrate material. Of these, the most important is that in the application of the coating, the substrate properties are not degraded. The current work in this direction has clearly shown that the preservation of substrate properties of a ceramic is exceedingly difficult.

It follows, then, that it becomes necessary to devise methods of applying energy-absorbing layers in a manner such that the required good adhesion of the layer to the SiC is achieved and, at the same time, the original surface of the SiC suffers no damage. Additionally, it becomes necessary to select material systems which will not chemically interact at the SiC/EAL interface. This is a most important consideration, especially under high-temperature operating conditions.

In examining this problem, an approach to the formation of high-temperature structural components equipped with an EAL has been found. The approach is to follow the concept that the ultimate component product will be fabricated in a one-step consolidation process. Further, it seeks to employ SiC throughout the material system with no second-phase materials present. In this way, the attendant problems with second materials present, such as chemical interactions, differences in thermal expansion, and bonding are completely avoided.

In the laboratory, it has been shown that if a sinterable SiC powder, such as that invented recently by Prochazka,\* is die-pressed and partially

---

\*"The Sintering of Silicon Carbide," S. Prochazka, Army Materials Technical Conference, Hyannis, MA, November 1973.

densified to form a "green" compact, then a layer of another SiC powder, in which densification in sintering has been inhibited, may be applied by a number of different methods. When the entire structure is sintered, the result is a duplex SiC body, the base of which is the fully sintered, dense, and strong SiC, and integrally bonded to it is a porous SiC layer. The porous layer is not only of interest from the standpoint of component protection and improved impact resistance, but also from the standpoint of improved performance in steep thermal gradients. Porous layers of the type described above are anticipated to exhibit thermal diffusivities 2 to 6 times lower than that for dense SiC and thus would act as thermal insulators to dense SiC substructures. Since porous bodies are characteristically more thermal-stress-resistant than dense bodies, the duplex SiC structures described above should exhibit improved performance in this respect.

In another segment of the overall program, it has been demonstrated that conventional, relatively inexpensive ceramic fabrication processes can be employed to form the desired component by the sintering technique. These include: die-pressing, injection-molding, extrusion, and slip-casting. With the planned approach of fabricating a duplex structure, although it has not as yet been attempted, it appears entirely feasible that they, too, could be fabricated by at least die-pressing, slip-casting, and extrusion. Perhaps the most attractive procedure will be to form the "green", partially sintered base article and to overlay it with the second SiC layer by spraying or any of a number of different application techniques.

Initial experiments featuring the formation of duplex, dense-porous structures have reduced the idea to practice.

Figure 17 shows the microstructure in the region where the dense SiC and the considerably porous (estimate 30% to 40% porosity) SiC were joined by sintering. This specimen was formed by simultaneously die-pressing two SiC powders, one being the fully sinterable powder to form the base ceramic. The other was a less sinterable SiC powder. The composite green body was then sintered according to established procedures.

Figure 18 shows the microstructure of a similar duplex structure. It was formed by making a "green" compact, by die-pressing a sinterable SiC powder, and applying the overlay of less sinterable powder by dipping the compact into a liquid suspension of the latter powder. When dry, the green body was sintered to develop the duplex microstructure.

Examination of both Figures 17 and 18 clearly reveals the duplex nature of the bodies. Although a general line of demarcation between dense and porous SiC can be distinguished, it is also evident that there is a continuous phase of dense SiC that connects the two structures. Porous overlays of SiC have been formed in thicknesses up to 2.29 mm by this method.

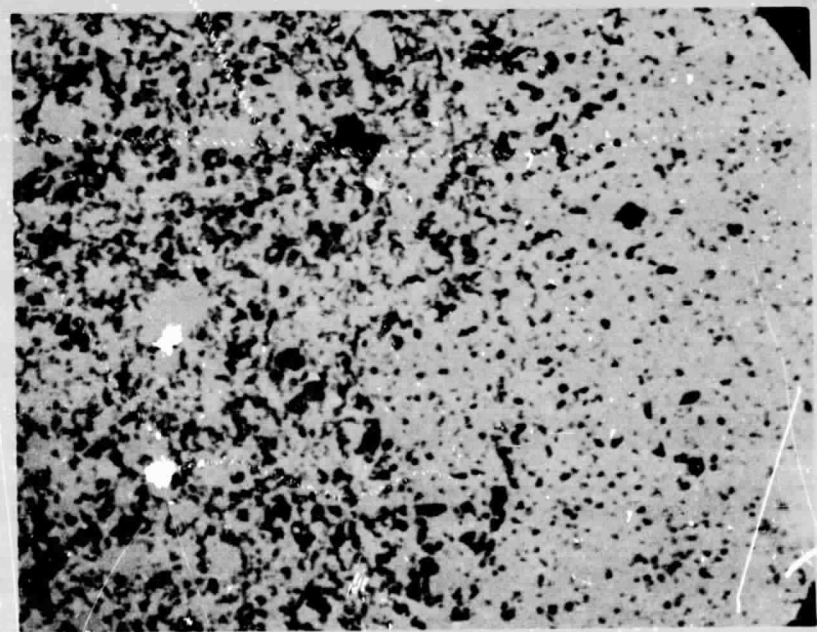


Figure 17. Transition Zone Between Dense and Porous SiC by Sintering Two Die-Pressed Powders 660X  
(1 cm = 15  $\mu$ m)

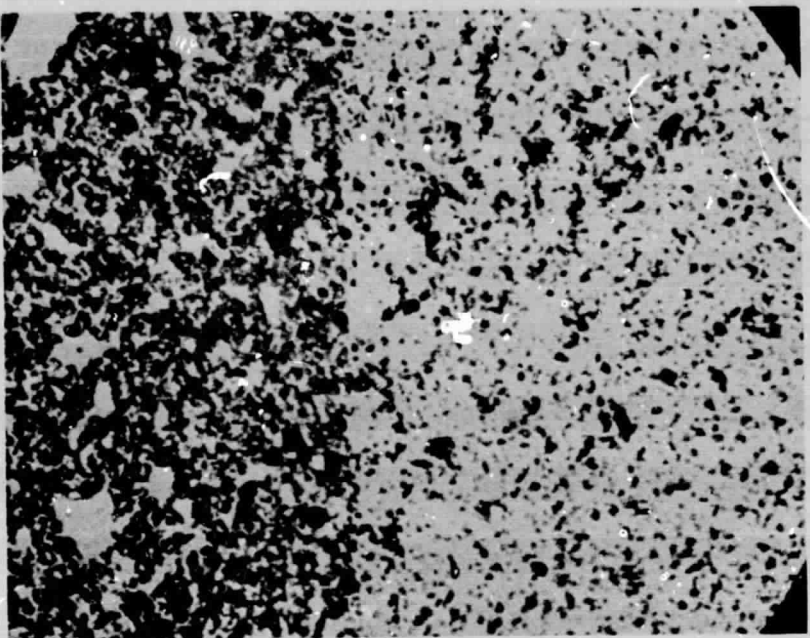


Figure 18. Transition Zone Between Dense and Porous SiC by Sintering Dipped Layer on Green Compact 660X  
(1 cm = 15  $\mu$ m)

Some initial base-line property data were determined on the Boron-doped cold-pressed and sintered SiC. Bend-test bars were die-pressed and sintered as described above, and three-point bend tests were conducted at room temperature. Results are shown in Table XII.

Table XII

THREE-POINT BEND TESTS ON SINTERED SiC  
(Test Bars Nominally 5.08 mm x 5.08 mm x 3.81 cm Span)

Test Specimen No.	Load	Bend Strength (R. T.) (MN/m <sup>2</sup> )
F-135	24.3	371
F-136	19.3	316
F-137	24.8	408
F-138	26.6	459
F-139	28.2	495

Sintered densities determined on the fractured pieces were found to average 2.97 gm/cc or about 92.5% of the theoretical value.

In the preparation of sinterable SiC powders, it is necessary to include about 0.3% E and an equally small amount of carbon in order to achieve acceptably high densities in the sintered product. Continued exploratory work has shown that triplex bar specimens, using SiC powders with varying amounts of added boron and carbon for the surface layers, can be fabricated. In one instance, a surface layer powder of SiC containing no added boron or carbon was sintered in place on the surface of the high density sintered core. Other surface layer powders containing small amounts of boron and carbon additives have yielded surface layer densities varying with the percentages of additives added. In all instances, the surface layers were integrally bonded to the center core.

Triplex bar specimens were fabricated by die pressing at 41 MN/m<sup>2</sup> and sintering between 2020°C and 2050°C for 15 minutes. Special die sets were made with die cavities having cross-sectional dimensions such that the as-pressed compacts would sinter and shrink to the required dimensions for both the standard bend-test bars and the Charpy impact test bars. Pressing and sintering the fully sinterable, or core powder alone, the volume shrinkage that takes place was found to be close to 46%. Linear shrinkage previously measured was found to be close to 17%.

Experiments were conducted to determine the density of the core or center layer of a triplex structure Charpy bar. In this instance, the two porous layers on opposing faces of the center layer were ground off and the density determined on the core. It was found, in two separate determinations to be 2.96 gm/cc or 92.2% of theoretical.

#### IV. SUMMARY OF RESULTS

1. Chemical treatment of the surface of hot-pressed SiC by fused salts treatment produces a thin porous surface, but mechanical strength is degraded. The room temperature fracture strength was reduced from 511 MN/m<sup>2</sup> to 345 MN/m<sup>2</sup> by a 30-minute immersion in a CaCl<sub>2</sub>-CaF<sub>2</sub>-CaSO<sub>4</sub> molten salt bath at 830°C. Fracture strength at 1325°C of the treated bars was 110 MN/m<sup>2</sup>.
2. Silicon was fusion-bonded to the surface of hot-pressed SiC. Careful control of the furnace atmosphere was necessary to achieve adhesion of the silicon. Oxidation of the silicon during processing resulted in nonuniform wetting of the SiC by the molten silicon.
3. Porous layers of aluminum oxide were applied to the surface of hot-pressed SiC. In order to achieve a reasonable degree of adhesion of the alumina to the substrate, the surface of the SiC was grit-blasted and plasma-spray coated with 0.025 mm of nickel aluminide. Fracture strengths at room temperature and at 1325°C were reduced to 70% of the as-machined material by the combined damage effects of the grit-blasting and the application of the nickel aluminide coating.
4. Charpy impact strengths of hot-pressed SiC were measured at room temperature and at 1325°C. Discrepancies amounting to a factor of 2 were noted in two sets of data taken on what should be expected to be the same material. Differences in the Charpy impact machine setup were thought to perhaps have altered the compliance of the machine. Subsequent tests on a second material disclosed little differences in results due to equipment differences.
5. Room temperature three-point bend strengths for hot-pressed SiC were found to be typically between 393 MN/m<sup>2</sup> and 511 MN/m<sup>2</sup> for these three different materials. The bend strength values at 1325°C for the same three materials varied from 248 MN/m<sup>2</sup> to 469 MN/m<sup>2</sup>. One of the three materials suffered a severe loss in strength (>50%) when tested at 1325°C, while the other two actually increased (5 to 8%).
6. Charpy impact tests were made with good reproducibility at 1325°C using a modified test machine and O<sub>2</sub>/H<sub>2</sub> gas torches for heating the specimen in place on the test machine.
7. Projectile impact damage (up to point of fracture by impact) to hot-pressed SiC was measured by three-point bend tests on the projectile damaged bar. Although the specimens were found to be capable of absorbing up to 0.2 Joules of projectile impact energy per cm<sup>3</sup> of specimen volume without fracture, severe bend strength degradation was observed to occur.

At 0.25 J/cm<sup>3</sup>, the specimen survival rate was only 20% and the bend strength of those that survived was only 138 MN/m<sup>2</sup>, an almost 4-fold reduction. Less energetic impacts resulted in measurably less damage to the body.

8. It was determined and generally concluded that although porous layers could be applied to hot-pressed SiC, sufficient damage was done in the processing to the SiC surface to drastically reduce its mechanical strength. It was further concluded that there was little if any chance of success in forming an effective energy-absorbing layer on the surface of fully densified SiC that would, at the same time, have the mechanical strength of the untreated or unsurfaced material.

9. Using General Electric pressureless sintering of SiC powders, it was discovered that porous layers of SiC could be formed on a dense, strong SiC substrate in a single consolidation process.

10. Room temperature three-point bend tests on General Electric fully densified by cold-press and sintering SiC typically were found to be close to 414 MN/m<sup>2</sup> (317-497) at densities of 2.97 gm/cc or 92.5% of theoretical.

## Appendix A

### HIGH TEMPERATURE CHARPY IMPACT TEST EQUIPMENT

Of some concern and the subject of considerable discussion in the early portion of the program was the method of running the high-temperature (1325°C) Charpy impact tests. It appeared that some sort of hot gas heating could be employed and the problems and time delays associated with the technique of containing the Charpy bar specimen in a furnace would be avoided. The one reservation held with regard to the heating of the test bar with hot gas was the uniformity of temperature across the entire length of the test bar. It was feared that the ends of the test bar would lose too much heat to the supports on which it rested and an excessive temperature gradient would exist from the center of the bar to each of its ends.

Using alumina ceramic, the structure of the Charpy machine was insulated to protect the throat of the machine as well as the upright supports and the hammer support and its bearings. Pyrolytic graphite was used to face the alumina blocks on which the test specimen rested. The pyrolytic graphite was shaped and placed in the equipment so that the test specimen was in contact with the AB planes of the graphite. Excessive heat loss out of the specimen was thus avoided, since the direction in the graphite normal to the two faces of the specimen was in the C or poor thermal conductivity direction. Two hydrogen-oxygen torches were fixed to direct the hot gases onto the specimen.

With a SiC test bar in place and heated to close to 1325°C, the temperature differences between the hottest and "coldest" section of the bar was 10° to 13°C, a variation from the established test temperature of less than 1%. Temperatures were measured by optical pyrometer and with a thermocouple placed in a hole drilled from one end of a bar into its center. Temperature measurements were cross-calibrated between the two techniques to factor out the effects of emissivity. Figure 19 shows the high-temperature assembly in operation with a standard 6.35 mm x 6.35 mm x 3.81 cm unnotched SiC test bar in place. This method of making Charpy impact tests on SiC at temperature proved to be rapid, easy to operate, reproducible in the values determined, and, as indicated above, with a minimum temperature variation across the test bar length, including the supported ends.

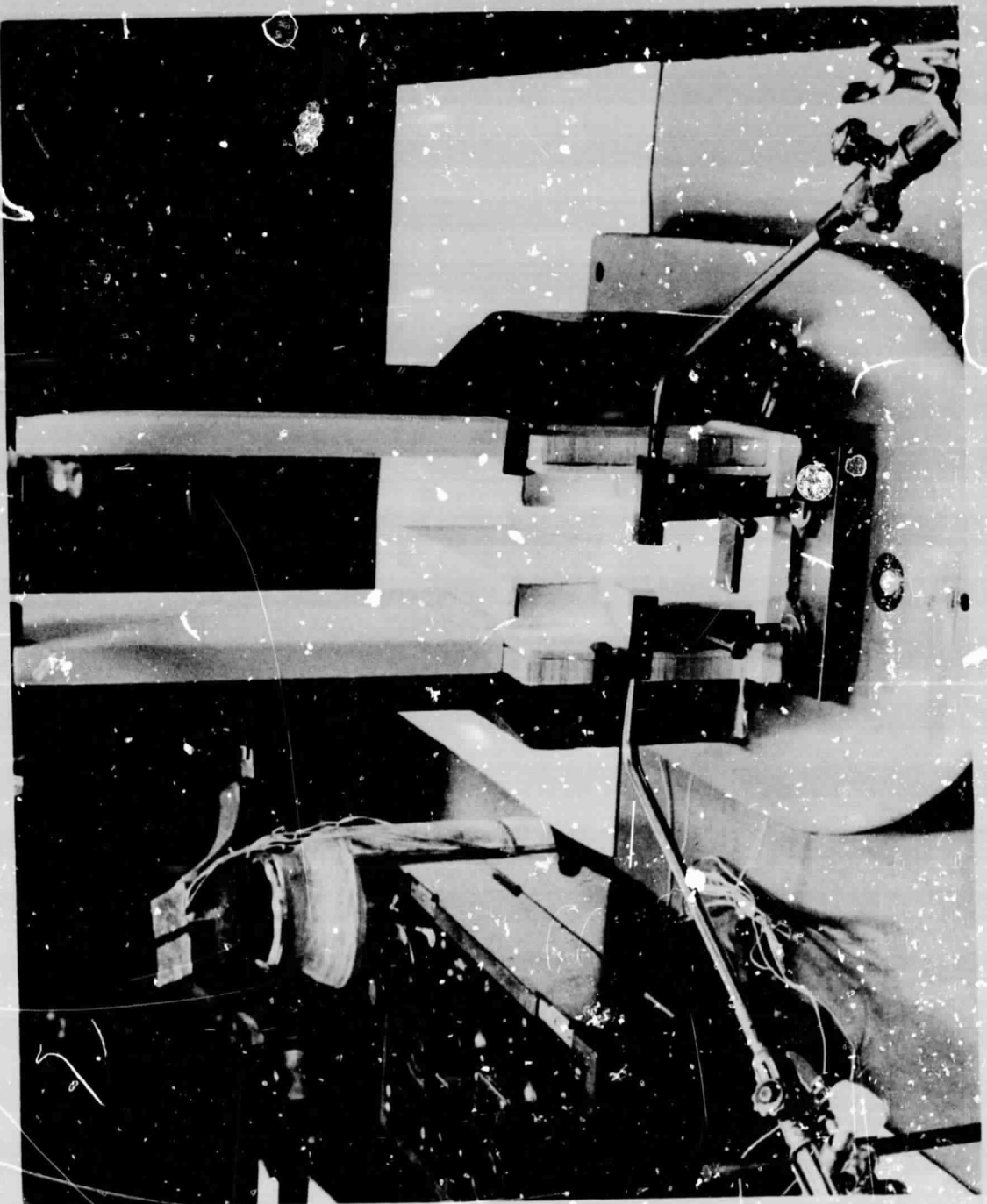


Figure 19. Charpy Impact Tester Assembled for Impact Determinations at 1325°C

## Appendix B

### PROJECTILE IMPACT TEST EQUIPMENT

In order to determine the degree of damage caused by projectile impact on SiC ceramic, it was proposed that this could be accomplished by impacting the surface of SiC with varying levels of impact energy and then to measure its bend strength; the greater the impact damage to the specimen, the lower should be its bend strength.

A test device was built to impart a projectile impact load (Figure 20) to SiC specimens. The device is simply one that allows a body of known weight to fall a measurable distance through an aluminum tube and to impact on the surface of the specimen. The head of the projectile (Figure 21) is a cone of tungsten carbide with its apex machined to a 1.587 mm radius. Teflon rings and guide bar minimize friction losses as the body falls through the aluminum tube.

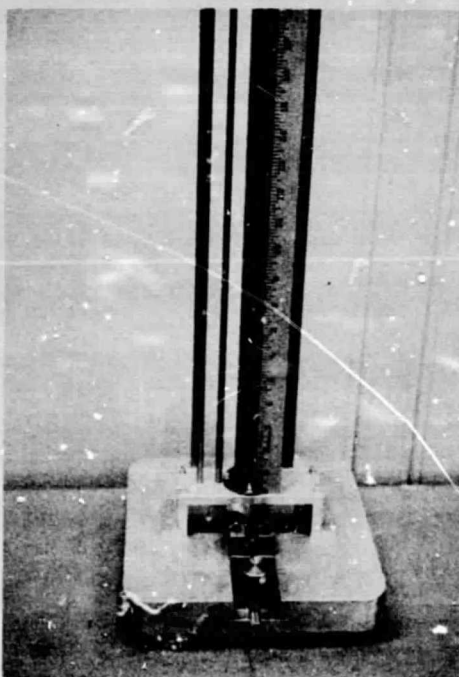


Figure 20. Base and Portion of Impact Device for Producing Hertzian-type Impact Damage in SiC Surface

Using the test device described above, five bend test bars of hot-pressed SiC were impacted at each of five different impact energies, including an energy level where 80% of the specimens ruptured on impact. Following this, the specimens were subjected to three-point bend test loading and bend strengths were determined for each group of five specimens.

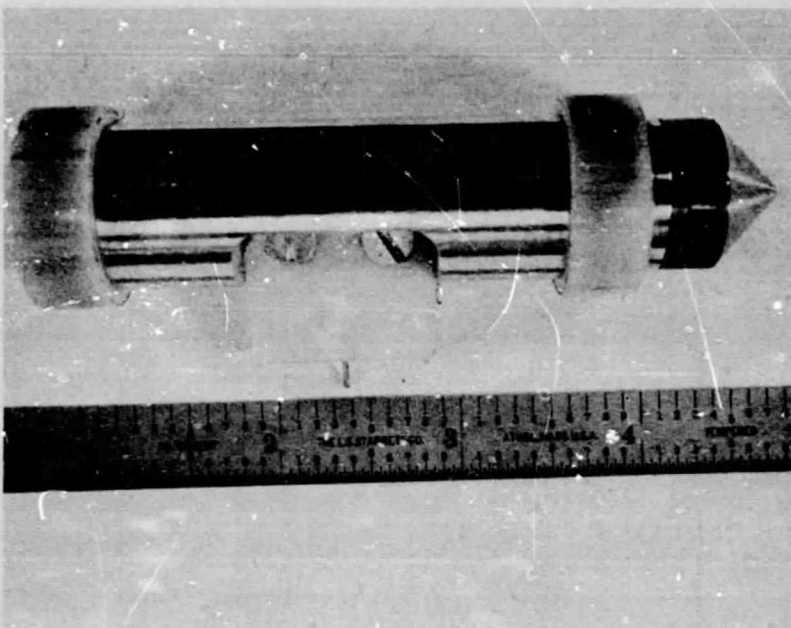


Figure 21. Falling Body Projectile Used to Produce Hertzian-type Impact Damage in Silicon Carbide Surface

Table XIII shows these data and Figure 22 is a plot of the data showing the loss in strength with increasing impact loading. The results of these determinations show a positive correlation between impact loading and bend strength, making it a useful tool for measuring impact damage.

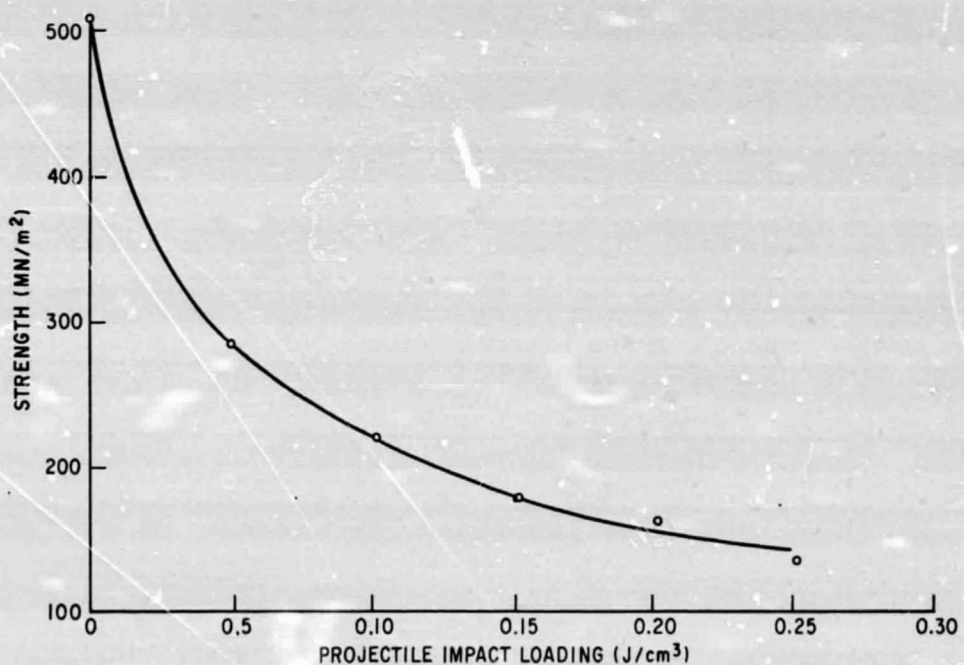


Figure 22. Strength vs Impact Loading Hot-Pressed SiC

Table XIII

THREE-POINT BEND STRENGTH ON PROJECTILE DAMAGED SPECIMENS  
 (Hot-Pressed SiC 5.08 mm x 2.54 mm x 3.81 cm Span)

Test Specimen No.	Impact Loading Joules/cm <sup>3</sup> Specimen Volume	Load to Fracture After Impact Damage (Kg)	Bend Strength After Impact Damage (MN/m <sup>2</sup> )
F 140	0.050	19.1	325
141	0.050	15.5	267
142	0.050	14.5	248
143	0.050	16.1	278
144	0.050	18.2	313
Average		-----	<u>286</u>
F 145	0.101	15.7	270
146	0.101	13.0	222
147	0.101	11.8	196
148	0.101	12.0	207
149	0.101	12.5	214
Average		-----	<u>222</u>
F 150	0.151	10.2	175
151	0.151	10.0	170
152	0.151	9.3	161
153	0.151	10.0	171
154	0.151	12.7	220
Average		-----	<u>179</u>
F 155	0.201	9.5	164
156	0.201	9.1	163
157	0.201	9.5	165
158	0.201	9.8	161
159	0.201	9.8	166
Average		-----	<u>164</u>
F 160*	0.251	8.0	136
161	0.251	8.0	138
Average		-----	<u>137</u>

\*8 other samples ruptured at this impact loading.